

Segregation-induced grain boundary premelting in nickel-doped tungsten

J. Luo,^{a)} V. K. Gupta, and D. H. Yoon^{b)}

School of Materials Science and Engineering and COMSET, Clemson University, Clemson, South Carolina 29634

H. M. Meyer III

High Temperature Materials Laboratory, Oak Ridge National Laboratory, Oak Ridge, Tennessee 37831

(Received 27 July 2005; accepted 20 October 2005; published online 28 November 2005)

High-resolution transmission electron microscopy and Auger spectroscopy have revealed the formation of nanometer-thick, Ni-enriched, disordered, grain boundary layers in Ni-doped W specimens at 95 °C below the bulk eutectic temperature. The stabilization of subeutectic liquid-like grain boundary cores in this model two-component metallic alloy is phenomenologically analogous to the long-sought phenomenon of grain boundary premelting. The existence of such disordered nanostructures at metallic grain boundaries provides insights to resolve several long-standing controversies in interpreting the unique grain boundary diffusion/migration kinetics and mechanical properties for this system, and can have technological importance for a broader range of materials. © 2005 American Institute of Physics. [DOI: 10.1063/1.2138796]

The existence of surface premelting,¹ first postulated by Faraday in 1860, is well-known now. In the 1980s, researchers also sought to confirm the existence of grain boundary (GB) premelting, wherein “liquid-like” layers are stabilized at GBs below the bulk melting temperature. Critical hot-stage transmission electron microscopy (TEM) experiments ultimately concluded that GB premelting likely occurred but only above $0.999T_{\text{melting}}$ for pure Al.² Further exploration in the area was greatly discouraged by this result. A most recent report³ provided clear evidence for the existence of GB premelting in colloidal crystals of submicron-size particles (as a model for atomic crystals of real materials).

Recent development in diffuse interface theories⁴ as a generalization of Cahn’s prewetting model⁵ suggests that liquid-like films can be stabilized at GBs in multicomponent systems over wider ranges of undercooling or undersaturation. Perhaps the most direct high-resolution transmission electron microscopy (HRTEM) evidence in this regard is the observations of subeutectic and subsolidus amorphous films of ~1 nm thick at GBs in Bi₂O₃-doped ZnO (Ref. 6) and (Y₂O₃+SiO₂)-doped Al₂O₃,⁷ as well as on free surfaces of several doped oxides.⁸ The existence of “equilibrium” intergranular amorphous films in ionic materials is well-known now,⁹ but the mechanism for these films to persist at conditions where a bulk liquid is no longer stable is rather controversial; it is possible that these liquid-like films are stabilized at GBs by a mechanism parallel to the premelting theory,^{6,8} wherein GB segregation and GB disordering promote each other.

More convincing evidence for the existence of segregation-induced GB premelting should be sought in simpler, non-glass-forming systems. Indeed, GB structural transitions in metallic alloys have been indirectly suggested by diffusivity anomalies and other macroscopic indications.¹⁰ Furthermore, the concept of segregation-induced GB pre-

melting is somewhat analogous to the segregation-induced polymorphous melting theory for GB embrittlement in S-doped Ni (see Ref. 11) that was recently proposed based on Auger spectroscopy and macroscopic properties. This study was motivated by the critical need of direct HRTEM plus Auger evidence for the existence of multilayer-adsorbed, disordered GBs in metals.

W–Ni has been chosen as the model metallic system because it has a simple binary eutectic phase diagram in the temperature range of interest [inset in Fig. 1(a)]¹² and exhibits enhanced GB diffusion behavior¹³ similar to ZnO–Bi₂O₃ which has been correlated with subeutectic amorphous GB films in a prior study.¹⁴ Furthermore, the high solid-state triple junction wetting temperature (~1450 °C, only slightly below $T_{\text{eutectic}}=1495$ °C) in W–Ni (see Ref. 15) offers a unique experimental opportunity. For specimens annealed at 1400 °C in this study, the secondary Ni-rich phase is present as scattered, isolated particles.¹⁵ Without the presence of a secondary crystalline phase at triple junctions as nuclei, it is difficult for Ni to diffuse out or fully crystallize upon cooling; thus the GB chemistry and structure are better preserved.

W powder (99.999%) was mixed with NiCl₂ (99.9998%) solution to dope with 0.05 to 1.0 at. % Ni. The mixture was dried, calcined, and compacted at ~80 MPa. The compacted pellets were sintered in flowing N₂+5% H₂ for 2 h at 1400 °C, and then cooled at ~30 °C/min in the protective gas. TEM specimens were prepared by ion milling with low incident angles to minimize milling damage. HRTEM was conducted using a 400keV JEOL 4000EX microscope. A special fixture was designed to fracture the specimens (intergranularly) *in situ* in UHV for scanning Auger electron spectroscopy in conjunction with Ar ion sputtering.

HRTEM images of a representative GB in a W+1 at. % Ni specimen prepared at 1400 °C are shown in Fig. 1. W lattice fringes are not contiguous at the GB, and a ~0.6-nm-thick intergranular layer is clearly identified. Careful alignment and focus adjustments ensured that the white layer is not a Fresnel fringe, with the observation of disordered structures within the film being additional direct proof. Despite indications of some local order existing within the film,

^{a)} Author to whom correspondence should be addressed; electronic mail: jianluo@clemson.edu

^{b)} Present address: School of Materials Science and Engineering, Yeungnam University, Korea.

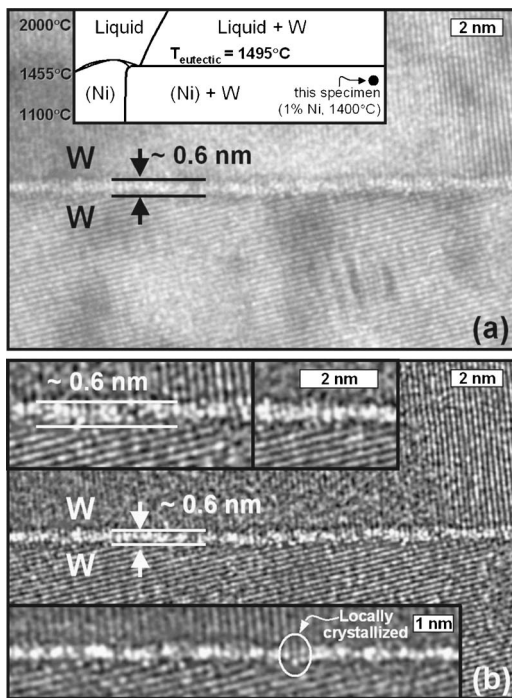


FIG. 1. (a) Original and (b) digitally enhanced HRTEM images of a disordered GB in a W+1 at. % Ni specimen annealed at 1400 °C. The inset in (a) is the W–Ni phase diagram (see Ref. 12), in which the specimen conditions are indicated. The two insets at the top-left corner of (b) are expanded views of selected regions; the inset at the bottom of (b) is an image of a different area. The digital enhancement process includes a background removal using fast Fourier transform pass band filtering with a $(2 \text{ nm})^{-1}$ aperture plus some brightness and contrast adjustments, which should not disturb any ordered or disordered features $<2 \text{ nm}$.

the intergranular layer is not fully crystallized. Furthermore, these GB layers cannot be the crystalline Ni phase because solid-state GB wetting does not occur in W–Ni at 1400 °C where the dihedral angle was found to be as great as 70° .¹⁵ Presumably, the formation of crystalline intergranular phase is frustrated by high interfacial energies for creating two crystal-to-crystal heterophase interfaces. The GB layers likely have become more ordered during cooling. The fact that these GB layers appear to be largely disordered in cooled specimens implies that the high temperature GB cores must be even more disordered and perhaps wider. These liquid-like GB layers occurred in a true solid-state equilibrium. Only two solid phases (Ni and W) are present between 1060 and 1495 °C [Fig. 1(a)],¹² excluding the possibility of solid-state amorphization.¹⁶

Figure 2(a) shows Ni/W ratio versus sputtering time, measured by Auger spectroscopy on fractured GBs for a specimen prepared at the same condition (1 at. % Ni, 1400 °C). The GB Ni segregation is clearly identified. The sputtering rate was calibrated to be 2 nm/min for a SiO₂ standard; hence, the width of Ni segregation region (0.5–1.0 nm if the material were SiO₂) is in a reasonable agreement with the HRTEM thickness of the disordered layer. The Ni-enriched composition of the disordered GB layer is also consistent with its brighter appearance in Fig. 1 due to atomic mass contrast.

GB chemistry was measured for a set of specimens containing 0.05–1.0 at. % Ni [Fig. 2(b)]. The observed plateau in Fig. 2(b) correlates well with the Ni solid-solubility limit in W.¹² The fact that GB Ni excess does not increase with the amount of secondary Ni-rich crystalline phases implies equi-

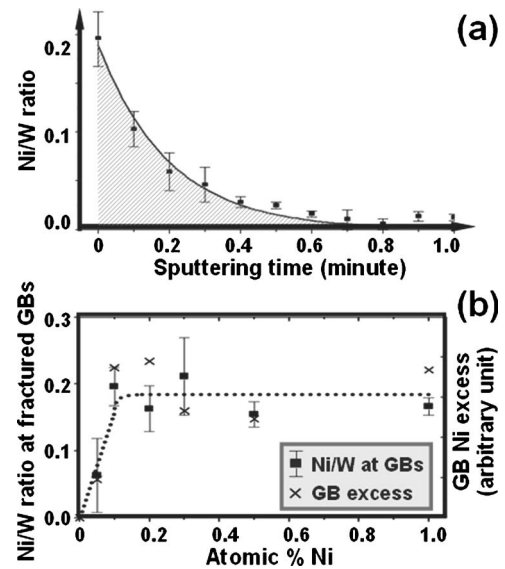


FIG. 2. (a) Ni/W ratio vs sputtering time for a W+1 at. % Ni specimen, annealed at 1400 °C. (b) Ni/W ratio at fractured GBs, and relative GB Ni excess, vs overall Ni content for specimens annealed at 1400 °C. The relative GB excesses are represented by the integrated area under Ni/W ratio vs sputtering time [e.g., the shaded area in (a)].

librium GB segregation for saturated specimens, and further confirms that the observed GB layer is not a complete wetting layer with a supply-controlled thickness.

The stabilization of a subeutectic, liquid-like, GB layer can be conceived if the increased free energy for forming the undercooled liquid layer ($\Delta G_{\text{amorph}}h$, h being the thickness) is more than compensated by the reduction in interfacial energies ($\gamma_{\text{gb}} - 2\gamma_{\text{cl}}$):

$$\Delta G_{\text{amorph}}h < \gamma_{\text{gb}} - 2\gamma_{\text{cl}} \equiv \Delta\gamma. \quad (1)$$

While the specific data of mixing entropy/enthalpy and interfacial energies are not available to fully evaluate Eq. (1), a simplified estimation can be made. The increased free energy for forming a 0.6-nm-thick, liquid-like layer of pure Ni at a 95 °C undercooling is estimated as

$$\Delta G_{\text{amorph}}h \approx \Delta S_{\text{fusion}}^{\text{Ni}} \Delta T (0.6 \text{ nm}) = 88 \text{ mJ/m}^2. \quad (2)$$

Since a perfect wetting of W GBs by the Ni-rich liquid phase (but not the Ni-rich crystalline phase) was evident near the eutectic temperature,¹⁷ $\Delta\gamma$ in Eq. (1) must be greater than zero but less than the W GB energy ($\gamma_{\text{gb}}^{\text{W}} = 1080 \pm 100 \text{ mJ/m}^2$ at 1500 °C¹⁸). If $\Delta\gamma$ is $>10\%$ of $\gamma_{\text{gb}}^{\text{W}}$, stabilization of this liquid-like GB layer can be rationalized thermodynamically. The fact that $\gamma_{\text{gb}}^{\text{W}} > 3\gamma_{\text{gb}}^{\text{Al}}$ ^{18,19} as well as a possible segregation effect,⁴ can be the reasons that GBs pre-melt over a much wider undercooling range in W–Ni than that in pure Al.²

The existence of disordered GBs explains several long-standing controversial observations. First, it was reported that $<1\%$ Ni addition will increase W GB diffusivities by $\sim 10^3$ times and therefore enhance solid-state sintering.¹³ This study suggests that rapid diffusion through disordered GB layers is responsible for this somewhat mysterious “solid-state activated sintering” phenomenon. This work and a prior study of a model oxide system ZnO–Bi₂O₃ (Ref. 14) demonstrated that bulk phase diagrams are not always accurate for predicting activated sintering systems, or in general, designing optimal material fabrication routes, as the classical

theories had often suggested, because the nanoscale interfacial phases do not follow bulk phase diagrams. Second, minor additions of Ni were found to promote rapid grain growth,²⁰ contrasting somewhat with the classical theory of solute drag to GB migration. This study suggests a new type of solute effect on GB migration, i.e., segregation enhances GB mobilities via promoting GB disordering. Finally, the Ni segregation causes GB embrittlement at room temperature but promotes plastic deformation at high temperatures,²¹ which can also be explained from the existence of liquid-like GB layers. Direct HRTEM observation of disordered GB cores in W–Ni supports the segregation-induced polymorphous melting theory for GB embrittlement,¹¹ even if the latter was initially proposed for Ni–S.

In summary, experiments using W–Ni as a model binary metallic system revealed the existence of nanometer-thick, Ni-enriched, liquid-like (disordered) GB layers at an undercooling of 95 °C. Despite the more extensive body of study of macroscopic indications of GB structural transitions,^{10,11} this result, to our knowledge, is the first direct HRTEM evidence for the existence of such disordered nanostructures at metallic GBs. This interfacial phenomenon is expected to occur in a broader range of multicomponent materials, where it can have heretofore unrecognized, yet important, roles in sintering, grain growth and mechanical/physical properties, especially for nanocrystalline materials.

This research is in part supported by a Clemson RGC award and an ORAU Ralph E. Powe Junior Faculty Enhancement award. Auger analysis was sponsored by the Assistant Secretary for Energy Efficiency and Renewable Energy, Office of Freedom Car and Vehicle Technologies, as part of the HTML User Program, ORNL, managed by UT-Battelle, LLC, for the U.S. DOE under Contract No. DE-AC05-00OR22725. The authors thank Dr. J. Hudson, Dr. Y. Ding, and Y. Berta for some assistance regarding TEM, and

Dr. R. M. Cannon and Professor Y.-M. Chiang for insightful discussions.

- ¹M. Faraday, Proc. R. Soc. London **330**, 599 (1860); J. G. Dash, Contemp. Phys. **30**, 89 (1989); J. G. Dash, H. Fu, and J. S. Wettlaufer, Rep. Prog. Phys. **58**, 115 (1995).
- ²T. E. Hsieh and R. W. Balluffi, Acta Metall. **37**, 1637 (1989).
- ³A. M. Alsayed, M. F. Islam, J. Zhang, P. J. Collings, and A. G. Yodh, Science **309**, 1207 (2005)
- ⁴A. E. Lobkovsky and J. A. Warren, Physica D **164**, 202 (2002); C. M. Bishop, M. Tang, R. M. Cannon, and W. C. Carter, Mater. Sci. Eng., A (submitted); M. Tang, W. C. Carter, and R. M. Cannon (unpublished).
- ⁵J. W. Cahn, J. Chem. Phys. **66**, 3667 (1977).
- ⁶H. Wang and Y.-M. Chiang, J. Am. Ceram. Soc. **81**, 89 (1998).
- ⁷I. MacLaren, R. M. Cannon, M. A. Gülgün, R. Voytovych, N. P. Pogrion, C. Scheu, U. Täffner, and M. Rühle, J. Am. Ceram. Soc. **86**, 650 (2003).
- ⁸J. Luo and Y.-M. Chiang, J. Eur. Ceram. Soc. **19**, 697 (1999); J. Luo and Y.-M. Chiang, Acta Mater. **48**, 4501 (2000); J. Luo, Y.-M. Chiang, and R. M. Cannon, Langmuir **21**, 7358 (2005).
- ⁹D. R. Clarke, J. Am. Ceram. Soc. **70**, 15 (1987); R. M. Cannon and L. Esposito, Z. Metallkd. **90**, 1002 (1999).
- ¹⁰J. Scholhammer, B. Baretzky, W. Gust, E. Mittemeijer, and B. Straumal, Interface Sci. **9**, 43 (2001); B. B. Straumal and B. Baretzky, *ibid.* **12**, 147 (2004).
- ¹¹J. K. Heuer, P. R. Okamoto, N. Q. Lam, and J. F. Stubbins, Appl. Phys. Lett. **76**, 3403 (2000); J. Nucl. Mater. **301**, 129 (2002).
- ¹²*Binary Alloy Phase Diagrams*, edited by T. B. Massalski (ASM International, Metals Park, OH, 1990), p. 2882.
- ¹³G. Flether, M. R. James, and J. R. Moon, Scr. Metall., **5**, 105 (1971); J. S. Lee, K. Klockgeter, and C. Herzig, Colloq. Phys., **51**, C1-569 (1990).
- ¹⁴J. Luo, H. Wang, and Y.-M. Chiang, J. Am. Ceram. Soc., **82**, 916 (1999).
- ¹⁵V. K. Gupta, D. H. Yoon, H. M. Meyer III, and J. Luo (unpublished).
- ¹⁶W. L. Johnson, *Materials Interfaces* (Chapman and Hall, New York, 1992), p. 517.
- ¹⁷Y. Liu, R. G. Iacocca, J. L. Johnson, R. M. German, and S. Kohara, Metall. Mater. Trans. A **26A**, 2484 (1993).
- ¹⁸E. N. Hodkin, M. G. Nicholas, and D. M. Poole, J. Less-Common Met. **20**, 93 (1970).
- ¹⁹L. E. Murr, *Interfacial Phenomena in Metals and Alloys* (Addison-Wesley, Reading, UK, 1975), p. 131.
- ²⁰I.-H. Moon, K.-Y. Kim, S.-T. Oh, and M.-J. Suk, J. Alloys Compd., **201**, 129 (1993).
- ²¹S.-W. Kim, S.-I. Lee, Y. D. Kim, and I.-H. Moon, Int. J. Refract. Met. Hard Mater. **21**, 183 (2003).